Acta Pharmacologica Sinica (2016) 37: 398–407
 1671-4083/16
www.nature.com/aps

Original Article

DW10075, a novel selective and small-molecule inhibitor of VEGFR, exhibits antitumor activities both *in vitro* and *in vivo*

Meng-yuan LI[1, 2, 4, #], Yong-cong LV[3, #], Lin-jiang TONG[2], Ting PENG[2], Rong QU[2, 4], Tao ZHANG[4, 5], Yi-ming SUN[2], Yi CHEN[2], Li-xin WEI[1, 4], Mei-yu GENG[2], Wen-hu DUAN[3, *], Hua XIE[2, *], Jian DING[2, *]

[1]*Pharmacology and Safety Evaluation Key Laboratory of Tibetan Medicine in Qinghai Province, Northwest Institute of Plateau Biology, Chinese Academy of Sciences, Xining 810008, China;* [2]*Division of Antitumor Pharmacology and* [3]*Department of Medicinal Chemistry, State Key Laboratory of Drug Research, Shanghai Institute of Materia Medica, Chinese Academy of Sciences, Shanghai 201203, China;* [4]*University of Chinese Academy of Sciences, Beijing 100049, China;* [5]*Shanghai Tech University, Shanghai 200120, China*

Aim: Targeting the VEGF/VEGF receptor (VEGFR) pathway has proved to be an effective antiangiogenic approach for cancer treatment. Here, we identified 6-((2-((3-acetamidophenyl)amino)pyrimidin-4-yl)oxy)-*N*-phenyl-1-naphthamide (designated herein as DW10075) as a novel and highly selective inhibitor of VEGFRs.

Methods: *In vitro* tyrosine kinase activity was measured using ELISA, and intracellular signaling pathway proteins were detected by Western blot analysis. Endothelial cell proliferation was examined with CCK-8 assays, and tumor cell proliferation was determined with SRB assays. Cell migration, tube formation and rat aortic ring assays were used to detect antiangiogenic activity. Antitumor efficacy was further evaluated in U87-MG human glioblastoma xenograft tumors in nude mice receiving DW10075 (500 mg·kg^{-1}·d^{-1}, *po*) for two weeks.

Results: Among a panel of 21 kinases tested, DW10075 selectively inhibited VEGFR-1, VEGFR-2 and VEGFR-3 (the IC_{50} values were 6.4, 0.69 and 5.5 nmol/L, respectively), but did not affect 18 other kinases including FGFR and PDGFR at 10 μmol/L. DW10075 significantly blocked VEGF-induced activation of VEGFR and its downstream signaling transduction in primary human umbilical vein endothelial cells (HUVECs), thus inhibited VEGF-induced HUVEC proliferation. DW10075 (1–100 nmol/L) dose-dependently inhibited VEGF-induced HUVEC migration and tube formation and suppressed angiogenesis in both the rat aortic ring model and the chicken chorioallantoic membrane model. Furthermore, DW10075 exhibited anti-proliferative activity against 22 different human cancer cell lines with IC_{50} values ranging from 2.2 μmol/L (for U87-MG human glioblastoma cells) to 22.2 μmol/L (for A375 melanoma cells). In U87-MG xenograft tumors in nude mice, oral administration of DW10075 significantly suppressed tumor growth, and reduced the expression of CD31 and Ki67 in the tumor tissues.

Conclusion: DW10075 is a potent and highly selective inhibitor of VEGFR that deserves further development.

Keywords: DW10075; VEGF/VEGF receptor inhibitor; antitumor; angiogenesis; U87-MG human glioblastoma

Acta Pharmacologica Sinica (2016) 37: 398–407; doi: 10.1038/aps.2015.117; published online 25 Jan 2015

Introduction

Angiogenesis, the formation of new blood vessels, is a crucial step for tumor survival, proliferation, invasion and metastasis. It is a highly complex process that is dependent on a multi-faceted program of endothelial cell activation, pro-angiogenic cytokine signaling, and activation of oncogenic signaling cascades[1, 2]. A key regulator of angiogenesis is the interaction of the vascular endothelial growth factor (VEGF) family of pro-angiogenic cytokines and their specific transmembrane receptors, VEGFRs. The VEGF family includes VEGF-A, -B, -C, -D, -E, and placental growth factor (PIGF) and three receptors: VEGFR-1 (Flt-1), VEGFR-2 (KDR) and VEGFR-3 (Flt-4)[3, 4]. Binding of VEGFs to VEGFRs initiates receptor dimerization and intracellular autophosphorylation of tyrosine residues with numerous downstream consequences. Downstream effects of VEGF/VEGFR signaling include a potent increase in vascular permeability and

[#]These authors contributed equally to this work.
[*]To whom correspondence should be addressed.
E-mail jding@simm.ac.cn (Jian DING);
hxie@simm.ac.cn (Hua XIE);
whduan@simm.ac.cn (Wen-hu DUAN)
Received 2015-09-17 Accepted 2015-10-28

endothelial cell proliferation, survival and migration, which ultimately result in neovascularization, tumor growth, and metastasis.

Overexpression of VEGFRs has been reported to correlate with the degree of vascularity, poor prognosis, and aggressive disease in the majority of human tumors[5]. Blocking VEGF/VEGFR signaling has become a promising approach for cancer therapy, and a number of VEGF/VEGFR-targeting agents have been approved for clinical treatment. The first drug that targeted VEGF signaling was Bevacizumab, which is a monoclonal neutralizing antibody of VEGF-A and has been approved for the treatment of renal cancer[6] and in combination with chemotherapy, for the treatment of metastatic colorectal cancer[7], metastatic breast cancer[8] and non-small-cell lung cancer (NSCLC)[9]. Moreover, a number of small-molecule inhibitors, such as sunitinib[10], sorafenib[11], pazopanib[12], cabozantinib[13], and regorafenib[14], have been developed and widely used in the treatment of hepatocellular carcinoma (HCC), gastrointestinal stromal tumor (GIST), soft tissue sarcoma (STS), medullary thyroid cancer (MTC) and metastatic renal cell carcinoma (RCC), either as a single agent or in combination with existing therapies[15]. Notably, most of these drugs inhibit VEGFR along with the blockade of other receptors, such as c-Kit, platelet-derived growth factor receptors (PDGFRs), fibroblast growth factor receptors (FGFRs) and Flt-3. Although multi-receptor tyrosine kinase (RTK) inhibitors can be highly effective in treating cancers by antagonizing more cancer targets, their off-target activities may lead to drug toxicity[16]. For example, hand-foot skin reactions, stomatitis, diarrhea, thyroid dysfunction and myelosuppression are commonly associated with treatment with multitargeted tyrosine kinase inhibitors (TKIs)[17]. The off-target effects of multitargeted TKIs have limited their use in combination regimens due to overlapping toxicities with other drugs and thus have led to the development of more selective and potent VEGFR inhibitors with the purpose of improving antitumor activity and decreasing off-target toxicity[18].

Recently, ramucirumab, a fully humanized IgG1 monoclonal antibody specifically targeting the extracellular domain of VEGFR-2, has received global approval by the US Food and Drug Administration (FDA) for clinical use[19, 20]. Axitinib, a pan-VEGFR inhibitor, and apatinib, a selective VEGFR-2 inhibitor, have also been approved by the US FDA and the China Food and Drug Administration (CFDA), respectively[21]. The approval of these inhibitors supports the idea that highly selective inhibition of VEGFR, particularly VEGFR-2, might be a promising, efficient, and safe approach to cancer treatment. Here, we report a novel highly selective VEGFR inhibitor DW10075, (6-((2-((3-acetamidophenyl)amino)pyrimidin-4-yl) oxy)-*N*-phenyl-1-naphthamide), which was obtained through a rationally designed kinase screen. DW10075 demonstrated potent inhibition of VEGFR-1, VEGFR-2, and VEGFR-3 kinase activity (nanomolar IC_{50}). It also exhibited dramatic anti-angiogenic effects both *in vitro* and *in vivo* and effectively suppressed tumor growth through antiangiogenic and anti-proliferative activity.

Materials and methods

Synthesis of DW10075

Unless otherwise noted, all starting materials and synthesis reagents were obtained commercially and used without further purification. Melting points (uncorrected) were measured on a Büchi B-510 melting point apparatus. ^{1}H NMR spectra were recorded on either a Varian Mercury 300 NMR or a Varian Mercury 400 NMR spectrometer. Chemical shifts are given in δ (ppm), and peak multiplicities are expressed as follows: s, singlet; d, doublet; dd, doublet of doublet; t, triplet; br s, broad singlet; m, multiplet. Low-resolution mass spectra (ESI) were recorded using an Agilent HPLC-MS (1260-6120B) spectrometer. High-resolution mass spectra (HRMS) were recorded on a Waters Q-Tof Ultima apparatus. The purity of DW10075 was determined on an Agilent Technologies 1260 series HPLC system using an Agilent Eclipse Plus column (C18, 4.6×150 mm, 3.5 μm).

6-((2-((3-acetamidophenyl)amino)pyrimidin-4-yl)oxy)-*N*-phenyl-1-naphthamide was designed and synthesized at the Shanghai Institute of Material Medica, Chinese Academy of Sciences. This compound was purified to achieve a purity of 99%.

6-(2-Chloropyrimidin-4-yloxy)-1-naphthoic acid (3)

1,8-Diazabicyclo (5,4,0)undec-7-ene (DBU, 4.8 mL, 31.88 mmol) was added dropwise to a stirred solution of 6-hydroxy-1-naphthoic acid (**1**, 2 g, 10.63 mmol) and 2,4-dichloropyrimidine (**2**, 3.17 g, 21.26 mmol) in 30 mL of dimethyl sulfoxide. The mixture was stirred at room temperature for 30 min. Ethyl acetate (300 mL) was added, and the mixture was extracted with 2 mol/L aqueous sodium hydroxide (3×60 mL). The aqueous layer was washed with ethyl acetate (2×60 mL) and then acidified with 6 mol/L hydrochloric acid to form a white suspension. The resulting precipitate was filtered, washed with water and vacuum-dried to yield **3,** a slightly yellow solid (1.92 g, 60%): mp: 210–212 °C; ^{1}H NMR (300 MHz, DMSO-d_6) δ (ppm): 7.28 (d, J = 6.3 Hz, 1H), 7.57 (dd, J = 9.6, 2.4 Hz, 1H), 7.63–7.68 (m, 1H), 7.93 (d, J = 2.4 Hz, 1H), 8.16-8.19 (m, 2H), 8.66 (d, J = 5.4 Hz, 1H), 8.97 (d, J = 9.3 Hz, 1H), 13.25 (br s, 1H); MS (ESI): 299.0 m/z $[M - H]^-$.

6-(2-((3-Acetamidophenyl)amino)pyrimidin-4-yloxy)-1-naphthoic acid (4)

Fifteen drops of concentrated hydrochloric acid were added to a solution of 6-(2-chloropyrimidin-4-yloxy)-1-naphthoic acid (**3**, 1.50 g, 4.99 mmol) and *N*-(3-aminophenyl)acetamide (1.12 g, 7.48 mmol) in isopropanol (60 mL), and the mixture was heated to reflux for 15 h. The mixture was cooled to room temperature and concentrated by vacuum. The residue was purified by silica gel column chromatography and eluted with methylene chloride/methanol/ethyl acetate (100: 2: 0.2) to yield **4** as a foam (1.55 g, 75%); ^{1}H NMR (300 MHz, DMSO-d_6) δ (ppm): 1.98 (s, 3H), 6.50 (d, *J* = 5.4 Hz, 1H), 6.78 (m, 1H), 7.11 (d, *J* = 7.2 Hz, 1H), 7.18 (d, *J* = 8.1 Hz, 1H), 7.54–7.69 (m, 3H), 7.89 (d, *J* = 2.4 Hz, 1H), 8.12–8.15 (m, 2H), 8.38 (d, *J* = 5.4 Hz, 1H), 8.97 (d, *J* = 9.3 Hz, 1H), 9.53 (s, 1H), 9.77 (s, 1H); MS (ESI):

413.1 m/z $[M - H]^-$.

6-(2-((3-acetamidophenyl)amino)pyrimidin-4-yloxy)-N-phenyl-1-naphthamide (DW10075)

Et_3N (5 mL, 36.20 mmol) was added to a solution of 6-(2-((3-acetamidophenyl)amino)pyrimidin-4-yloxy)-1-naphthoic acid (**4**, 1 g, 2.41 mmol) and aniline (330 μL, 3.62 mmol) in 10 mL *N*,*N*-dimethylformide, followed by propylphosphonic anhydride (50% propylphosphonic anhydride in ethyl acetate, 4.3 mL, 7.24 mmol) and 4-dimethylaminopyridine (147 mg, 1.21 mmol). After the mixture was stirred for 5 h, water (80 mL) was added to form a white suspension. The resulting precipitate was filtered, washed with water and vacuum-dried to yield DW10075, a white solid (827 mg, 70%): mp: 237-239 °C; ^{1}H NMR (400 MHz, DMSO-d_6) δ (ppm): 1.98 (s, 3H), 6.50 (d, *J*=5.6 Hz, 1H), 6.84 (m, 1H), 7.14 (t, *J*=7.2 Hz, 2H), 7.19-7.21 (m, 1H), 7.39 (t, *J*=7.6 Hz, 2H), 7.54 (dd, *J*=8.8, 2.4 Hz, 1H), 7.64-7.68 (m, 2H), 7.78-7.80 (d, *J*=6.8 Hz, 1H), 7.83 (d, *J*=7.6 Hz, 2H), 7.91 (d, *J*=2.4 Hz, 1H), 8.09 (d, *J*=8.4 Hz, 1H), 8.29 (d, *J*=9.6 Hz, 1H), 8.38 (d, *J*=5.6 Hz, 1H), 9.56 (s, 1H), 9.80 (s, 1H), 10.64 (s, 1H); HRMS (ESI) m/z calcd for $C_{29}H_{23}N_5O_3Na$ $[M+Na]^+$: 512.1699, found: 512.1702.

In vitro kinase assays

The ability of DW10075 to inhibit the activity of a panel of kinases was tested using an enzyme-linked-immunosorbent assay (ELISA) *in vitro*. The kinase domains of VEGFR-1, VEGFR-2, and VEGFR-3 were expressed using the Bac-to-Bac™ baculovirus expression system (Invitrogen, Carlsbad, CA, USA). Recombinant ErbB2, ErbB4, RET, EGFR, c-Kit, EGFR/T790M/L858R, ABL, EPH-A2, PDGFR-α, FGFR1, FGFR2, IR, FGFR3, FGFR4, BTK, FAK, Tie2, JAK1, JAK2, JAK3 and IGF1R proteins were obtained from (Lake Placid, NY, USA). The 96-well ELISA plates were coated with substrate, which contains 20 μg/mL Poly (Glu, Tyr)$_{4:1}$ (Sigma, St Louis, MO, USA). The experiment was performed according to standard ELISA procedures, and the plate was read at an absorbance of 490 nm. The inhibitory rate (%) was calculated using the following formula: [1- (A_{490}treated/A_{490}control)] × 100%. IC_{50} values were calculated from the inhibitory curves[22].

Endothelial cell proliferation

Primary human umbilical vein endothelial cells (HUVECs) were obtained from PromoCell (Heidelberg, Germany) and cultured in Endothelial Cell Growth Medium 2. To determine the percentage of inhibition of endothelial proliferation stimulated by VEGF, HUVECs were plated into 96-well plates at 5500 per well and starved for 24 h after attachment. Different concentrations of compounds were added 2 h before the addition of 100 ng/mL recombinant human $VEGF_{165}$ (PeproTech EC, Ltd, London, United Kingdom), and the cells were incubated at 37 °C in a CO_2 incubator for 48 h. The effects on proliferation were determined using the Cell Counting Kit-8 (CCK-8) assay (Dojindo Molecular technologies Inc, Shanghai, China). Ten microliters of CCK-8 were added to each well, and the plate was incubated for 4 h at 37 °C in a CO_2 incubator; the amount of formazan dye generated by cellular dehydrogenase activity was measured using a multi-well spectrophotometer (VERSA max™, Molecular Devices, Sunnyvale, CA, USA) at an absorbance of 450 nm. The inhibitory rates (%) of compounds were calculated with the following formula: [1-($A_{450\ treated}/A_{450\ control}$)]×100%. IC_{50} values were calculated from the inhibitory curves.

Western blot analysis

HUVECs were seeded to six-well plates at 40000 cells per well. Cells were washed three times with PBS after adherence to remove serum protein, and cells were then starved with serum-free medium for 24 h. Different concentrations of DW10075 were added to the wells, and the cells were then incubated for 6 h before stimulation by 100 ng/mL $VEGF_{165}$ per well. Cells were washed, and whole-cell lysates for Western blotting were extracted with RIPA (25 mmol/L Tris-HCl pH 7.6, 150 mmol/L NaCl, 1% NP-40, 1% sodium deoxycholate, 0.1% SDS, protease, and phosphatase inhibitor cocktail). Cell lysates (30 μg) were loaded onto an SDS-PAGE gel and transferred to a polyvinylidene fluoride membrane. The anticipated objective strap position on the membrane was cliped, and the membrane was incubated overnight at 4 °C with the following antibodies: p-VEGFR-2 (Tyr1175), VEGFR, p-AKT (Ser473), AKT, p-ERK(Thr202/Thr204), ERK and GAPDH (Cell Signaling Technologies, Cambridge, MA, USA). Western blot analysis was subsequently performed with standard procedures.

Cell migration assay

HUVECs resuspended in Endothelial Cell Basal Medium at a density of 2×10^5 cells/mL were seeded (0.1 mL) in the plate inserts of the transwell chamber (pore size 8 μm; Corning Life Sciences, Lowell, MA), and in the well below, Endothelial Cell Basal Medium (0.6 mL) containing 100 ng/mL VEGF with or without various concentrations of DW10075 was added. HUVECs were subsequently cultured for 24 h. Cells that migrated to the lower wells were then fixed by 90% ethanol, stained by 0.1% crystal violet, and photographed. The crystals stained on the lower side of the well were dissolved by 100 μL of 10% acetic acid, and the absorbance of the resulting solution was measured at 600 nm using a multiwell spectrophotometer (SpetraMAX 190; Molecular Devices, Sunnyvale, CA). The group stimulated only by VEGF was used as a positive control. The relative migration was calculated as ($OD_{Treated}/OD_{VEGF}$)×100%[23].

Tube formation assay

HUVECs were starved with Endothelial Cell Basal Medium for 24 h before being placed on 96-well plates. The plates were coated with 60 μL Growth Factor Reduced (GFR) Standard BD Matrigel matrix (BD Biosciences, Billerica, USA) per well and incubated at 37 °C. The BD Matrigel matrix is a reconstituted basement membrane preparation that consists of approximately 60% laminin, 30% collagen IV, and 8% entactin. GFR BD Matrigel matrix contains <0.5 ng/mL EGF, <0.2 ng/mL

NGF, <5 pg/mL PDGF, 5 ng/mL IGF-1 and 1.7 ng/mL TGF-β; a low concentration of growth factor is for applications that benefit from a more highly defined basement preparation. HUVECs were digested by 0.04% trypsin-EDTA, and digestion was terminated by 3% BSA, then centrifuged at 800 r/min for 3 min to remove trypsin and serum, and cells were resuspended in Endothelial Cell Basal Medium. Cells were plated on coated 96-well plates at 20000 cells per well, and different concentrations of DW10075 and $VEGF_{165}$ (final 100 ng/mL) were added. To make sure that the tubes were driven by VEGF, there was a VEGF-free group that showed different results compared with the positive control. Plates were incubated for 6 h at 37 °C in a CO_2 incubator until the tube network formed completely. Photographs were then taken through a stereoscope (OLYMPUS IX51) at 4× magnification. The experiment was repeated at least three times independently to detect the effects of DW10075 on endothelial tube formation.

Rat aortic ring assay

The rat aortic rings were obtained from 6-week-old Sprague-Dawley rats. Each aorta was cut into 1 mm slices, which were embedded in 75 μL Matrigel per well in 96-well plates, incubated with M199 medium containing 10% FBS and various concentrations of DW10075, and then photographed on day 7 with an inverted phase contrast microscope (IX-51, Olympus, Japan)[24]. The capillaries were quantified based on the relative area covered by capillaries using Image-Pro Express.

Chicken chorioallantoic membrane (CAM) assay

Ten fertilized chicken eggs were incubated in a humidified egg incubator (Lyon Electric Company, CA, USA) that was maintained at 37 °C and 50% humidity; eggs were allowed to grow for seven days. Gentle suction was applied at the hole located at the broad end of the egg to create a false air sac directly over the chicken chorioallantoic membrane, and a 1 cm^2 window was removed from the egg shell immediately afterwards. Glass coverslips (0.5×0.5 cm) saturated with DW10075 or normal saline were placed on areas between preexisting vessels, and the embryos were further incubated for 48 h. The neovascular zones beside the glass coverslips were photographed under a stereomicroscope (MS5; Leica, Heerbrugg, Switzerland). Vessel branches were observed in five random views of less than 3 mm.

Tumor cell viability assays

Tumor cell viability was evaluated using the SRB (Sulforhodamine B) assay. Cells were seeded onto 96-well plates at 3000–6000 cells per well and cultured overnight to allow for adherence. They were then treated with different concentrations of DW10075 and incubated for 72 h. The medium was removed immediately after 72 h, and 100 μL 10% precooled trichloroacetic acid was added per well at 4 °C (TCA) as a fixative. Fixed cells were left on the plate at 4 °C for 1 h; then plates were washed five times with distilled water and dried. Cells were stained with 4 mg/mL SRB solution (Sigma, St Louis, MO, USA) prepared with 1% acetic acid; 100 μL was added to each well for 15 min, and then plates were washed five times with a 1% acetic acid solution and dried. The stain was dissolved using 10 mmol/L Tris-HCl. One hundred fifty microliters were added per well, and plates were read at 560 nm using a multi-well VersaMax spectrophotometer (Molecular Devices, Sunnyvale, CA, USA). The rate of inhibition of cell proliferation was calculated by the following: $[1-(A_{560\ treated}/A_{560\ control})]\times 100\%$. The IC_{50} values were calculated by the Logit method. The final data were based on the average results of at least three independent tests.

In vivo anti-tumor activity

Six male BALB/cA nude mice were housed per cage for group administration. Mice were 5–6 weeks old, and the initial weight was 22±2 g. Animal experiments were performed according to the institutional ethical guidelines of animal care. Cell lines were obtained from the American Type Culture Collection (Manassas, VA, USA). U87-MG cells were injected sc into the right flank of each mouse at a density of 5×10^6 in 200 μL, and the resulting tumors were allowed to grow to 600 mm^3, which was defined as a well-developed tumor. The well-developed tumors were cut into 1.5 mm^3 fragments and transplanted sc into the right flanks of nude mice using a trocar. When the tumor volume reached 200 mm^3, the mice were randomly assigned into control and treatment groups (n=6 per group). Control groups were given vehicle alone, and treatment groups received 500 mg/kg oral doses of DW10075 once daily for two weeks. Tumor sizes and animal weights were measured twice per week using a microcaliper and weight scale, respectively. The tumor volume (V) was calculated as follows: $V=0.5\times$[length (mm)×width^2 (mm^2)]. The individual relative tumor volume (RTV) was calculated as follows: $RTV=V_t/V_0$, where V_t is the volume on each day, and V_0 represents the volume at the beginning of the treatment. RTV was shown on indicated days as the mean±SD indicated for groups of mice. Inhibition of solid tumor growth on a specific day or tumor size was represented as the mean volume of the DW10075 group over the mean volume of the untreated group by T/C or as percent inhibition of the control T/C $(\%)=(T_{RTV}/C_{RTV})\times 100\%$.

Immunohistochemistry

Tumor samples were fixed in formalin for over 24 h, transferred to 70% ethanol, and embedded in paraffin wax. Sections (5 μm) were cut and baked onto microscope slides. The slides were incubated with primary CD31 and Ki67 antibodies (Epitomics, Burlingame, CA, USA) and then secondary antibodies and visualized using a colorimetric method (DAB kit; ZSGB-Bio, Beijing, China). Stained sections were imaged using a BX51 Olympus microscope and a Microfire Digital Camera (Olympus).

Statistical analysis

All final values were presented as the mean±SD. Statistical analysis (t test) was performed using the SPSS 22.0 software. Differences were determined to be significant when $P<0.05$.

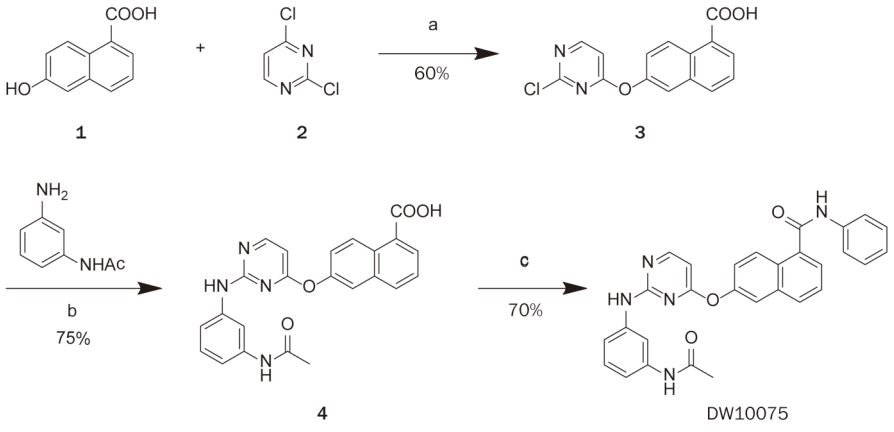

Figure 1. Synthesis of DW10075. Reagents and conditions: (a) DBU, DMSO, rt; (b) HCl, i-PrOH, reflux; (c) $PhNH_2$, T3P, Et3N, DMAP, DMF, rt.

Results

Chemistry

The synthesis of DW10075 is shown in Figure 1A. Pyrimidine-containing intermediate **3** was prepared by substituting dichloropyrimidine **2** with 6-hydroxy-1-naphthoic acid (**1**) in the presence of DBU at room temperature. Subsequent condensation with *N*-(3-aminophenyl)acetamide in isopropanol with a catalytic amount of hydrochloric acid yielded anilinopyrimidine **4**. Treatment of **4** with *N*-(3-aminophenyl)acetamide in the presence of T3P yielded DW10075.

DW10075 potently and selectively inhibits VEGFR *in vitro* kinase activities

Because DW10075 was designed to be a potential VEGFR inhibitor, we first evaluated the activity of DW10075 against the three members of the VEGFR family, using an ELISA kinase assay with human recombinant enzymes. In concentration-dependent experiments, DW10075 potently and dose-dependently inhibited the kinase activities of the VEGFRs. The IC_{50} values of this compound against VEGFR-1, VEGFR-2 and VEGFR-3 were 6.4, 0.7, and 5.5 nmol/L, respectively (Table 1). To identify other potential targets of DW10075, a kinase profile assay was conducted and a panel of 21 other kinases, including VEGFR highly homologous kinases FGFR1, FGFR2 and PDGFR-α, were examined. DW10075 exhibited no inhibitory activity against the kinases, even at a much higher concentration (10 μmol/L) compared with an untreated control (Table 1). The results indicated that DW10075 is a highly selective inhibitor that targets VEGFR family members, particularly VEGFR-2.

DW10075 selectively inhibits VEGF-mediated endothelial cell survival by suppressing VEGFR activation and its downstream signaling transduction

The potency of DW10075 against VEGF-mediated endothelial cell proliferation was further assessed using primary human umbilical vein endothelial cells (HUVECs), which express high levels of VEGFRs. As shown in Figure 2A, DW10075 markedly inhibited the VEGF-stimulated proliferation of HUVECs in a dose-dependent manner, with an IC_{50} value of 3.9 nmol/L. We also compared the efficacy of DW10075 on the proliferation of HUVECs, mediated by fetal bovine serum (FBS) or by different types of growth factors, including VEGF, basic fibroblast growth factor (bFGF) and platelet-derived growth factor (PDGF). DW10075 showed more potent inhibition of VEGF-induced proliferation than that mediated by 10% FBS, bFGF or PDGF (Figure 2B). Thus, these results continue to support DW10075 as a selective inhibitor of VEGFR.

We then investigated the target inhibition of DW10075 in

Table 1. DW10075 kinase selectivity profile.

Tyrosine kinase	IC_{50} (nmol/L)	Tyrosine kinase	IC_{50} (nmol/L)
VEGFR-1	6.4±0.4	ErbB4	>10 000
VEGFR-2	0.7±0.3	EGFR/T790M/L858R	>10 000
VEGFR-3	5.5±1.2	ABL	>10 000
FGFR1	>10 000	EPH-A2	>10 000
FGFR2	>10 000	IR	>10 000
FGFR3	>10 000	BTK	>10 000
FGFR4	>10 000	FAK	>10 000
PDGFR-α	>10 000	Tie2	>10 000
c-Kit	>10 000	JAK1	>10 000
RET	>10 000	JAK2	>10 000
ErbB2	>10 000	JAK3	>10 000
EGFR	>10 000	IGF1R	>10 000

The IC_{50} values are shown as the mean±SD and estimated values from three independent experiments. VEGFR, vascular endothelial growth factor receptor 2; FGFR1, fibroblast growth factor receptor 1; PDGFR, platelet-derived growth factor receptor; c-Kit, tyrosine-protein kinase kit; RET, rearranged during transfection tyrosine kinase; ErbB, human epidermal growth factor receptor; EGFR, epidermal growth factor receptor; ABL, abelson murine leukemia viral oncogene homolog 1; EPH-A2, ephrin type-A receptor 2; IR, insulin receptor; JAK, janus kinase; Tie2, tyrosine kinase with immunoglobulin-like and EGF-like domains 2; IGF1R, insulin-like growth factor 1 receptor.

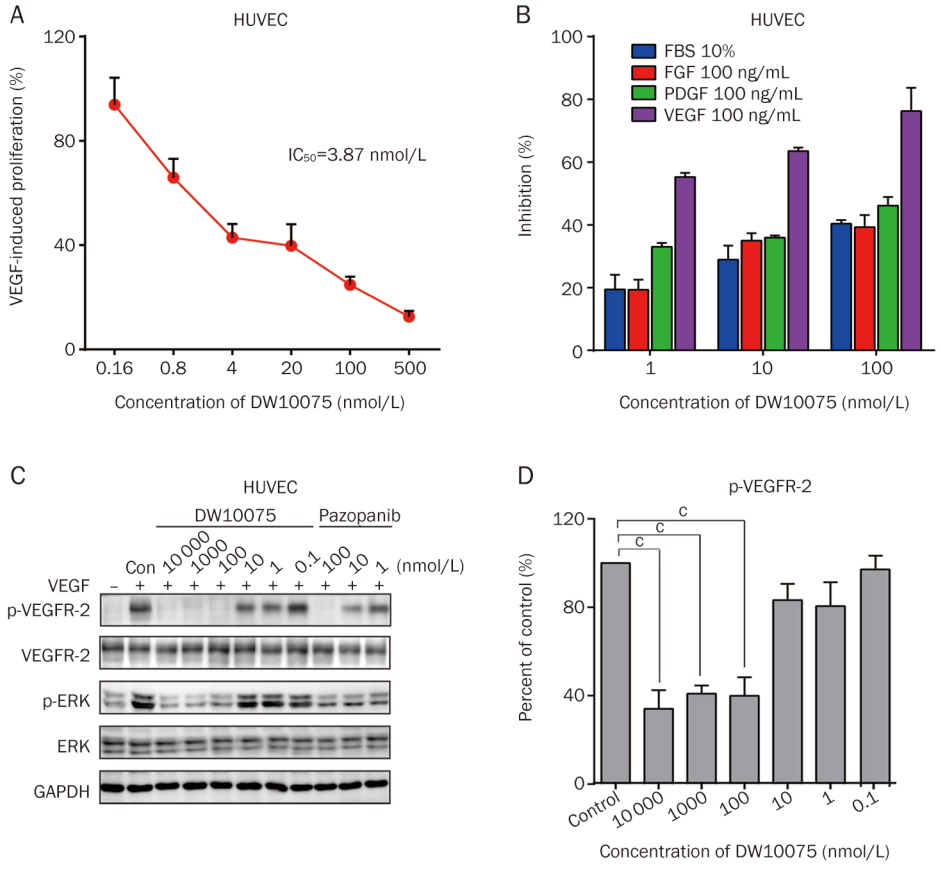

Figure 2. DW10075 selectively inhibits VEGF-mediated endothelial cells survival through suppressing the activation of VEGFR and its downstream signaling transduction. (A) DW10075 against VEGF-mediated endothelial cells survival. The effects on proliferation were determined by CCK-8 assay and values represented the average of three repeats. (B) The effect of DW10075 on other growth factor-mediated endothelial cells survival. There are significant difference in FBS, FGF and PDGF group compared to VEGF-stimulated group. (C) DW10075 blocks intracellular VEGFR-2 signal transduction in endothelial cells. DW10075 effectively inhibits the phosphorylation of VEGFR-2 and the ERK1/2, a downstream member of VEGFR-2 pathway, in VEGF-stimulated HUVEC cells. (D) Qualitative analysis of the signal transduction blocks effect of DW10075 on HUVEC cells. Mean±SD. *n*=3. $^{c}P<0.01$ *vs* vehicle control.

HUVECs. As shown in Figure 2C, DW10075 dramatically and dose-dependently inhibited VEGF-induced phosphorylation of VEGFR-2 at the Tyr1175 phosphorylation sites. A very low concentration of DW10075 (1 nmol/L) caused a 19.4% inhibition of VEGFR-2 phosphorylation, and 100 nmol/L of DW10075 resulted in a 60.1% inhibition. In accordance with the observation of p-VEGFR-2 suppression, the phosphorylation of ERK (Thr202/204), one of the key molecules downstream of VEGFR, was also significantly inhibited by DW10075 (Figure 2C and 2D). Together, these results clearly show that DW10075 potently inhibits the activation of VEGFR and its downstream signaling transduction and thus inhibits the proliferation of HUVECs.

DW10075 showed potent antiangiogenic activity both *in vitro* and *in vivo*

As VEGF/VEGFR signaling is critical in the process of angiogenesis, we further detected the antiangiogenic activity of DW10075 *in vitro* and *in vivo*. The migration and formation of functional tubes in HUVECs plated on Matrigel were assessed. As illustrated in Figure 3A and 3B, DW10075 treatment suppressed VEGF-induced HUVEC migration and tube formation in a dose-dependent manner. At a concentration of 100 nmol/L, DW10075 suppressed 61.8% of HUVEC migration and 54.3% of tube formation.

We further tested the antiangiogenic activity of DW10075 using an aortic ring assay and a CAM assay, which are *ex vivo* and *in vivo* methods, respectively, that recapitulate the key steps in the angiogenesis process. The results of the aortic ring assay are shown in Figure 3C. DW10075 showed potent inhibition of capillary formation in the rat aortic ring (75.9% and 96.8% inhibition at 10 and 100 nmol/L, respectively). The results of the CAM assay (Figure 3D) showed that neovascularization in chick embryos was significantly inhibited after DW10075 treatment, and the inhibition was 42.5%, 86.5% and 95.7% at concentrations of 1, 10 and 100 nmol/L, respectively. Together, these results indicated that as an inhibitor targeting VEGFRs, DW10075 potently inhibits angiogenesis both *in vitro* and *in vivo*.

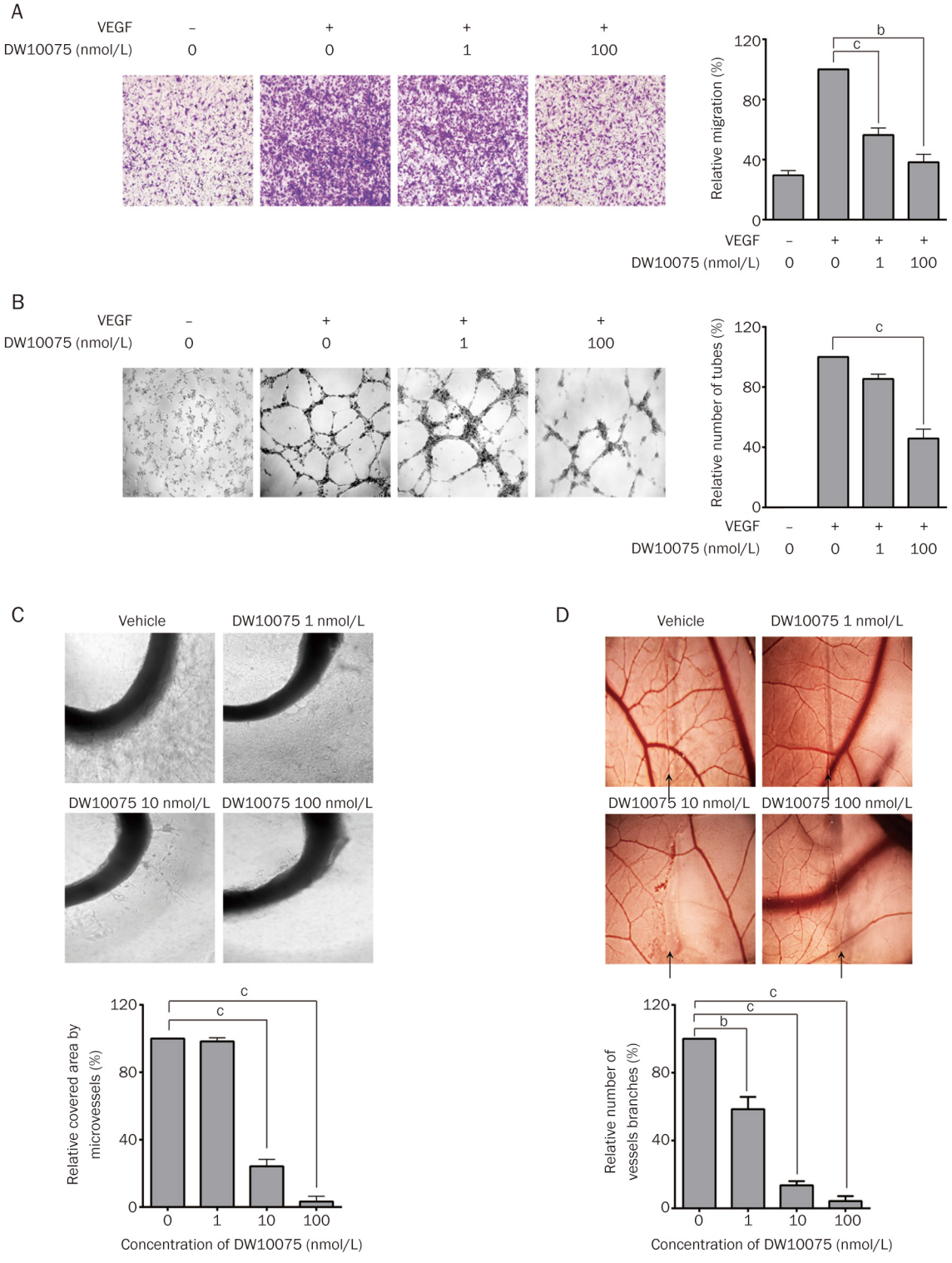

Figure 3. DW10075 showed potent antiangiogenesis activity both *in vitro* and *in vivo*. (A) DW10075 blocks the migration of HUVEC induced by VEGF. After cultured for 24 h the cells that migrated to the lower wells were then fixed and photographed. Quantitative analysis of the effect on migration of different concentrations of DW10075 is on the right. (B) DW10075 blocks VEGFR-dependent tube formation. To make sure the tubes were driven by VEGF, there is a VEGF-free group showing different results compared with positive control. Quantitative analysis of the destructive effect on tube network of different concentrations of DW10075 is on the right. (C) DW10075 suppressed vessels sprouting from the rat aorta rings. Images were taken by an inverse microscope. Quantitative analysis of the destructive effect on rat aortic ring angiogenesis of DW10075 is shown in the lower panel. (D) DW10075 inhibits angiogenesis on the CAM model. The neovascular angiogenesis was limited by DW10075 at 10 nmol/L. Quantitative analysis of the destructive effect on CAM angiogenesis of DW10075 is shown in the lower panel. Mean±SD. n=3. $^{b}P<0.05$, $^{c}P<0.01$ *vs* vehicle control.

DW10075 suppressed the *in vitro* proliferation of a panel of tumor cells

We next sought to address whether DW10075 possessed anti-proliferative activity using the SRB assay against a panel of human tumor cell lines. We found that DW10075 inhibited the proliferation of different types of tumor cells with IC_{50} values ranging from 2.2 μmol/L (for U87-MG glioma cells) to 22.2 μmol/L (for A375 melanoma cells) (Figure 4A). The IC_{50} values of DW10075 to inhibit the proliferation of cancer cells are 600- to 6000-fold greater than those required for comparable inhibition of VEGF-stimulated HUVEC proliferation. Therefore, the results showed that DW10075 could inhibit the *in*

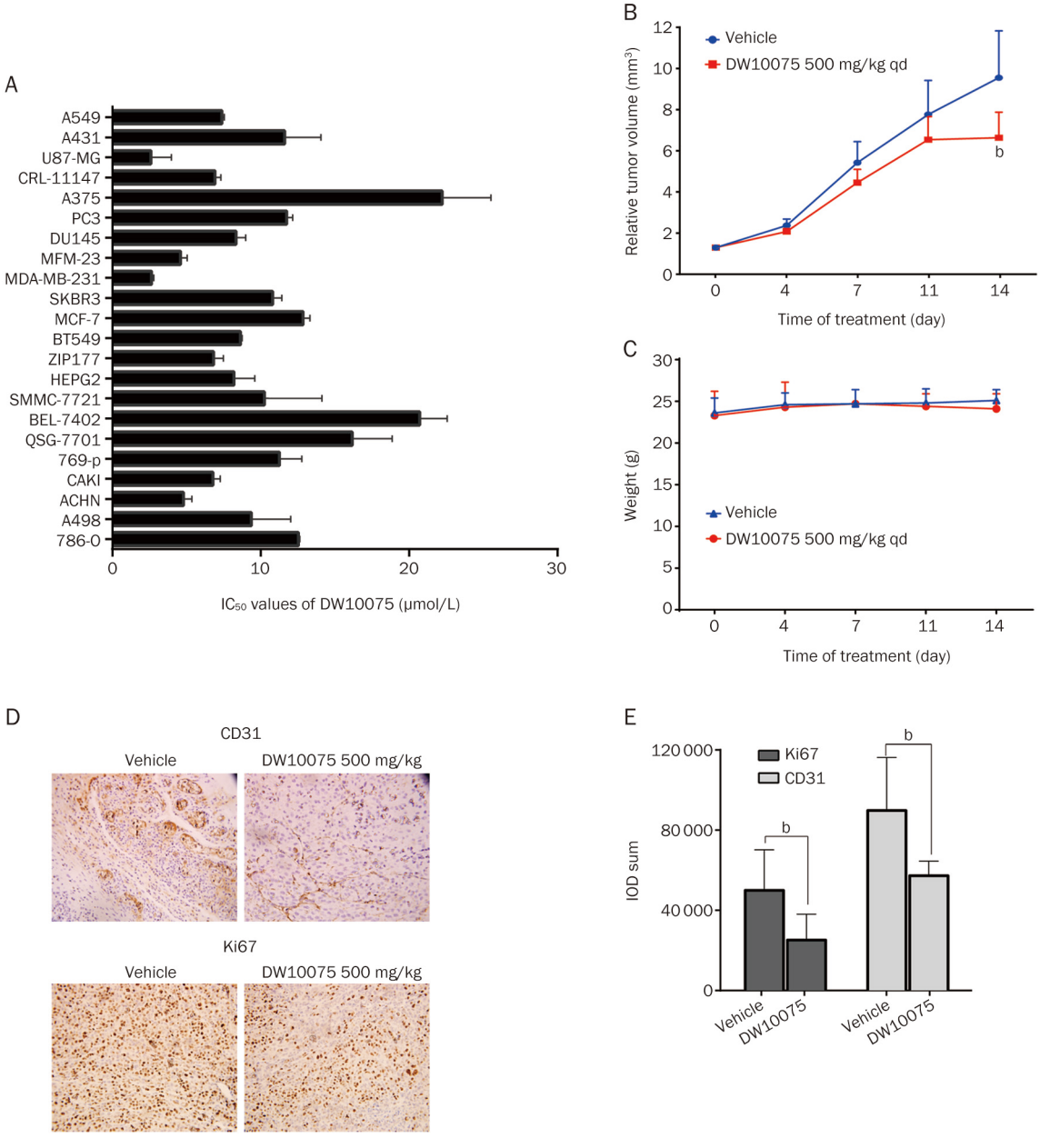

Figure 4. DW10075 suppressed the *in vitro* proliferation of a panel of tumor cells and exerts antitumor activity in U87-MG xenograft tumor in nude mice model through anti-angiogenetic and anti-proliferative effects. (A) DW10075 could inhibit the growth of tumor cells *in vitro*, but need much higher concentration. The IC_{50} values of DW10075 are plotted as the mean±SD and all estimated values are from three independent experiments. (B) DW10075 inhibits growth of U87-MG human glioblastoma tumors in nude mice. Tumor volume was measured on the indicated days with the mean tumor volume indicated for groups. (C) DW10075 had no distinct impact on the weight of treated group animals. Mean weight±SD were shown and the initial weight is 22±2 g, following the treatment of DW10075 for 14 d, the weight is still kept in this range. (D) The expression of CD31 and Ki67 were significant reduced in the 500 mg/kg *po* qd DW10075 group in the U87-MG xenograft. Evaluation of CD31 and Ki-67 expression in tumor tissue of treated or vehicle control groups by IHC on d 14. (E) Quantitative analysis of the CD31 and Ki67 expression in the 500 mg/kg *po* qd DW10075 group in the U87-MG xenograft. The quantity of the expression was evaluated by IOD sum using Image-Pro Express. Mean±SD. n=3. $^bP<0.05$ *vs* vehicle control.

vitro growth of tumor cells, but a much higher concentration is needed.

DW10075 exerts antitumor activity in U87-MG xenograft tumors in nude mice through antiangiogenic and anti-proliferative effects

Given the encouraging antiangiogenic and anti-proliferation activity *in vitro*, we then evaluated the antitumor efficacy of DW10075 *in vivo*. An U87-MG glioblastoma xenograft model was used here because U87-MG cells showed the highest sensitivity to DW10075 *in vitro* (Figure 4A). The results showed that tumor growth was suppressed in mice treated with 500 mg/kg DW10075 once-daily *po*, leading to a T/C% of 69.6% (Figure 4B). After administration of DW10075 for two weeks, statistically significant inhibition of tumor growth ($P<0.05$) was observed on the 14th day. Meanwhile, the weight of the experimental animals was not significantly reduced, indicating that DW10075 was well tolerated by the mice (Figure 4C).

Moreover, intratumoral CD31, a marker of angiogenesis, was subsequently examined using immunohistochemistry (IHC). As shown in Figure 4D and 4E, intratumoral CD31 was inhibited after oral administration of 500 mg/kg DW10075, clearly indicating that oral treatment with DW10075 effectively suppressed angiogenesis in xenograft tumors. Intratumoral Ki67, a proliferation marker, was also measured. The results showed that Ki67 expression was significantly decreased in the 500 mg/kg DW10075 group (Figure 4D and 4E), indicating that DW10075 had anti-proliferative activity *in vivo*. These results suggest that both the antiangiogenic and the anti-proliferative activity of DW10075 contributed to the *in vivo* antitumor activity of this compound.

Discussion

Given the importance of angiogenesis in cancer progression, it is not surprising that considerable effort has been made to interfere with this process, particularly VEGF/VEGFR-mediated signaling, in cancer treatments. VEGF/VEGFR-targeting anti-tumor therapy has been developed for over 30 years, and several inhibitors, including monoclonal antibodies, multi-kinase inhibitors and selective VEGFR inhibitors, have been approved and widely used in the treatment of various types of cancer[15, 25]. Although multi-RTK inhibitors showed satisfactory results in the treatment of cancer, the off-target effects, serious side effects and complicated mechanism limited the clinical application of multi-RTK inhibitors, both in single-agent and combination therapies. Therefore, the development of next-generation VEGFR TKIs with much higher selectivity and improved potency has the potential to provide more effective and better tolerated treatment options, enabling the development of rationally designed combination therapies. Several highly selective VEGFR inhibitors have already been used in the clinic, and more are currently in different stages of preclinical and clinical development. Axitinib is the first FDA-approved highly selective inhibitor of VEGFRs, and it shows similar potency against VEGFR-1, VEGFR-2 and VEGFR-3 (IC_{50} values at 0.1–0.3 nmol/L). It also exhibits potent inhibition of PDGFR and moderate inhibition of RET and other kinases[26]. Apatinib is a highly selective VEGFR-2 inhibitor that was approved for the treatment of gastric cancer in China in 2014. In addition to VEGFRs, apatinib also exhibits moderate inhibition of RET, c-kit, and c-Src[27]. In this report, we identified DW10075 as a novel, highly selective inhibitor of VEGFRs that is almost equally as potent as axitinib and apatinib. Notably, it showed no inhibition of the *in vitro* activity of the 21 kinases tested, including highly homologous kinases FGFRs and PDGFRα, even at much higher concentrations. Therefore, DW10075 is a novel, highly selective and potent inhibitor of VEGFRs and deserves further investigation.

Intriguingly, our results demonstrated that DW10075 showed approximately 7- to 9-fold greater potency against VEGFR-2 (IC_{50} 0.7 nmol/L) compared with VEGFR-1 and VEGFR-3 (IC_{50} 6.4 and 5.5 nmol/L, respectively). Of the three VEGFR family members, VEGFR-2 seems to mediate the major mitogenic, angiogenic, and permeability-enhancing effects of VEGF. VEGFR-2 is not only the key regulator of tumor angiogenesis, but it also contributes to the function of cancer stem cells and tumor initiation[28]. By contrast, VEGFR-1 exhibits high binding affinity for VEGF-A, but its weak phosphorylation suggests a negative modulatory role on VEGF signaling, and VEGFR-3 is primarily involved in lymphangiogenesis. Therefore, development of novel inhibitors that selectively inhibit VEGFR-2 but not the other VEGFR family members might be an attractive approach for cancer therapy[3]. Our results demonstrate that DW10075 exhibits selective inhibition against VEGFR-2 with high potency, which is even lower than apatinib, as reported previously (IC_{50} 1 nmol/L)[27], clearly indicating that DW10075 possesses comparable VEGFR-2 inhibitory activity and much higher selectivity than the known selective VEGFR inhibitors.

Our data also demonstrated that DW10075 dose-dependently inhibited the VEGF-induced phosphorylation of VEGFR-2 and its downstream signaling transduction and thus, markedly reduced HUVEC proliferation in response to VEGF. In addition, DW10075 inhibited the migration and tube formation of HUVECs and suppressed angiogenesis in the aortic ring and CAM models. These results clearly demonstrated that as a selective VEGFR inhibitor, DW10075 possessed potent antigiogenetic activities. Moreover, it inhibited the proliferation of a panel of tumor cells. The anti-proliferative effects required a DW10075 dose (IC_{50} 2.2 to 22.2 μmol/L) that was much higher than that required to inhibit the proliferation of HUVECs and suppress angiogenesis. *In vivo* studies further confirmed that both antiangiogenic and anti-proliferative activities contributed to the anti-tumor effects of DW10075, as evidenced by the reduced expression of CD31 and Ki67. It is noteworthy that although DW10075 exhibits excellent target inhibitory activity, as well as potent antiangiogenic efficacy *in vitro*, it has only moderate *in vivo* anti-tumor activity. One of the potential explanations might be that the pharmacokinetic (PK) characteristics of DW10075 might not be good enough. Therefore, further evaluation of the PK profile of this compound is needed, and this may be useful for further modification of its preparation and structure.

We have identified DW10075 as a novel and highly selective inhibitor of VEGFRs. Its significant antiangiogenic and anti-tumor activities both *in vitro* and *in vivo*, combined with a convenient synthetic approach and good solubility, make DW10075 a promising agent in cancer therapy.

Acknowledgements

This work was financially supported by the National Natural Science Foundation of China (No 81173080, 81321092 and 81374063), the National Key Technology R&D Program of the Ministry of Science and Technology of China (2012BAI27B02) and the Research Program of Qinghai province (No 2012-T-Y23).

Author contribution

Meng-yuan LI, Yong-cong LV, Mei-yu GENG, Wen-hu DUAN, Hua XIE, and Jian DING designed the research; Meng-yuan LI, Yong-cong LV, Li-xin WEI, Lin-jiang TONG , Yi CHEN, Wen-hu DUAN, Hua XIE performed the research; Meng-yuan LI, Yong-cong LV, Ting PENG, Rong QU, Tao ZHANG, and Yi-ming SUN contributed new reagents or analytic tools; Meng-yuan LI, Yong-cong LV, and Hua XIE analyzed the data; Meng-yuan LI, Yong-cong LV, Wen-hu DUAN, and Hua XIE wrote the manuscript.

References

1 Weis SM, Cheresh DA. Tumor angiogenesis: molecular pathways and therapeutic targets. Nat Med 2011; 17: 1359–70.
2 Potente M, Gerhardt H, Carmeliet P. Basic and therapeutic aspects of angiogenesis. Cell 2011; 146: 873–87.
3 Ferrara N, Gerber H-P, LeCouter J. The biology of VEGF and its receptors. Nat Med 2003; 9: 669–76.
4 Bergers G, Benjamin LE. Tumorigenesis and the angiogenic switch. Nat Rev Cancer 2003; 3: 401–10.
5 Goel S, Duda DG, Xu L, Munn LL, Boucher Y, Fukumura D, *et al*. Normalization of the vasculature for treatment of cancer and other diseases. Physiol Rev 2011; 91: 1071–121.
6 Willett CG, Boucher Y, Di Tomaso E, Duda DG, Munn LL, Tong RT, *et al*. Direct evidence that the VEGF-specific antibody bevacizumab has antivascular effects in human rectal cancer. Nat Med 2004; 10: 145–7.
7 Giantonio BJ, Catalano PJ, Meropol NJ, O'Dwyer PJ, Mitchell EP, Alberts SR, *et al*. Bevacizumab in combination with oxaliplatin, fluorouracil, and leucovorin (FOLFOX4) for previously treated metastatic colorectal cancer: results from the Eastern Cooperative Oncology Group Study E3200. J Clin Oncol 2007; 25: 1539–44.
8 Gray R, Bhattacharya S, Bowden C, Miller K, Comis RL. Independent review of E2100: a phase III trial of bevacizumab plus paclitaxel versus paclitaxel in women with metastatic breast cancer. J Clin Oncol 2009; 27: 4966–72.
9 Sandler A, Gray R, Perry MC, Brahmer J, Schiller JH, Dowlati A, *et al*. Paclitaxel–carboplatin alone or with bevacizumab for non–small-cell lung cancer. N Engl J Med 2006; 355: 2542–50.
10 Chow LQ, Eckhardt SG. Sunitinib: from rational design to clinical efficacy. J Clin Oncol 2007; 25: 884–96.
11 Iyer R, Fetterly G, Lugade A, Thanavala Y. Sorafenib: a clinical and pharmacologic review. Expert Opin Pharmacother 2010; 11: 1943–55.
12 Bukowski RM, Yasothan U, Kirkpatrick P. Pazopanib. Nat Rev Drug Discovery 2010; 9: 17–8.
13 Traynor K. Cabozantinib approved for advanced medullary thyroid cancer. Am J Health Syst Pharm 2013; 70: 88.
14 Andre T, Dumont SN. Regorafenib approved in Metastatic Colorectal cancer. Bull Cancer 2013; 100: 1027–9.
15 Ivy SP, Wick JY, Kaufman BM. An overview of small-molecule inhibitors of VEGFR signaling. Nat Rev Clin Oncol 2009; 6: 569–79.
16 Shepard DR, Garcia JA. Toxicity associated with the long-term use of targeted therapies in patients with advanced renal cell carcinoma. Expert Rev Anticancer Ther 2009; 9: 795–805.
17 Kumar R, Crouthamel MC, Rominger DH, Gontarek RR, Tummino PJ, Levin RA, *et al*. Myelosuppression and kinase selectivity of multikinase angiogenesis inhibitors. Br J Cancer 2009; 101: 1717–23.
18 Bhargava P, Robinson MO. Development of second-generation VEGFR tyrosine kinase inhibitors: current status. Curr Oncol Rep 2011; 13: 103–11.
19 Spratlin J. Ramucirumab (IMC-1121B): Monoclonal antibody inhibition of vascular endothelial growth factor receptor-2. Curr Oncol Rep 2011; 13: 97–102.
20 Poole RM, Vaidya A. Ramucirumab: first global approval. Drugs 2014; 74: 1047–58.
21 Ho TH, Jonasch E. Axitinib in the treatment of metastatic renal cell carcinoma. Future Oncol 2011; 7: 1247–53.
22 Peng T, Wu JR, Tong LJ, Li MY, Chen F, Leng YX, *et al*. Identification of DW532 as a novel anti-tumor agent targeting both kinases and tubulin. Acta Pharmacol Sin 2014; 35: 916–28.
23 Chen LK, Qiang PF, Xu QP, Zhao YH, Dai F, Zhang L. Trans-3, 4, 5, 4′-tetramethoxystilbene, a resveratrol analog, potently inhibits angiogenesis *in vitro* and *in vivo*. Acta Pharmacol Sin 2013; 34: 1174–82.
24 Aplin AC, Nicosia RF. The rat aortic ring model of angiogenesis. Methods Mol Biol 2015; 1214: 255–64.
25 Rao N, Lee YF, Ge R. Novel endogenous angiogenesis inhibitors and their therapeutic potential. Acta Pharmacol Sin 2015; 36: 1177–90.
26 Hu-Lowe DD, Zou HY, Grazzini ML, Hallin ME, Wickman GR, Amundson K, *et al*. Nonclinical antiangiogenesis and antitumor activities of axitinib (AG-013736), an oral, potent, and selective inhibitor of vascular endothelial growth factor receptor tyrosine kinases 1, 2, 3. Clin Cancer Res 2008; 14: 7272–83.
27 Tian S, Quan H, Xie C, Guo H, Lü F, Xu Y, *et al*. YN968D1 is a novel and selective inhibitor of vascular endothelial growth factor receptor-2 tyrosine kinase with potent activity *in vitro* and *in vivo*. Cancer Sci 2011; 102: 1374–80.
28 Goel HL, Mercurio AM. VEGF targets the tumour cell. Nat Rev Cancer 2013; 13: 871–82.